ORAL/POSTER REFERENCE: ICF100985OR

# INFLUENCE OF RESIDUAL STRESS ON DUCTILE CRACK INITIATION AND GROWTH IN DISSIMILAR METAL WELD JOINTS

A. H. Sherry, D. P. G. Lidbury and D. W. Beardsmore

AEA Technology plc, Risley, Warrington, WA3 6AT, UK

## ABSTRACT

BIMET was a European programme concerned with the structural integrity of components containing dissimilar metal welds. Led by EDF, the BIMET group was composed of eight European partners. Working under the Fourth Framework programme of Nuclear Fission Safety of the European Atomic Energy Community (EURATOM), the group has made significant progress in developing analytical methods for assessing defect behaviour in weldments joining ferritic and austenitic components. These developments have taken place with reference to two benchmark tests. Each test featured a dissimilar metal weld joining austenitic and ferritic pipe material, with the whole assembly tested in four point bending at ambient temperature. An external EDM (electro-discharge-machine) notch was inserted into the SA308 stainless steel weld metal buttering layer, within 2 mm of the ferritic steel pipe and in a region of high weld residual stress. The defect orientation led to combined Mode I and II loading at the crack tip. This paper presents a detailed R6-based analysis of the BIMET 01 and 02 tests, with particular emphasis on the role of residual stress on crack initiation and subsequent crack growth behaviour. The results demonstrate the importance of taking proper account of residual stresses within structural integrity assessments.

## KEY WORDS

Dissimilar metal welds, residual stresses, R6, structural integrity, defect assessment

## INTRODUCTION

The BIMET (Structural Integrity of Bi-Metallic Components) project was carried out for the European Commission under the Euratom 4$^{th}$ Framework Programme. Eight European partners were involved: EDF (Project Co-ordinator), JRC-IAM Petten, AEA Technology, TWI, GKSS, VTT, Framatome, and CEA. The objective of the project was to contribute to the development and validation of analytical methods used to assess the behaviour of defects located at dissimilar metal welds (DMW). The principal focus was two large-scale benchmark tests, each featuring a 4-point bend test of a nominal 6-inch (152 mm) piping assembly, which contained a ferritic to stainless steel DMW, Figure 1. In each test, a pre-crack was machined within the ferritic/buttering layer to simulate PWR plant experience of cracking in components containing such welds.

Defects in DMWs provide significant challenges to integrity assessment procedures since they include a variation in material properties across the weld, mixed-mode loading and significant residual stresses. This paper presents the results from R6 analyses of the BIMET01 and 02 tests. The R6 procedure [1] includes guidance on the treatment of weld mismatch, mixed-mode loading and residual stresses in defect assessment. Analyses of these tests thus provide a valuable basis on which to validate R6.

## BIMET01 AND 02 TESTS

The BIMET01 and 02 test assemblies consisted of 200mm long A508 ferritic steel and type 304 stainless steel sections joined via a DMW carried out to ASME specification, Figure 1. The outside diameter of the specimen was 168mm and the wall thickness (t) was 25mm. Straight-fronted, part-penetrating defects were inserted from the outer surface into the first buttering layer (309L) adjacent to the buttering/ferritic steel interface and inclined to run parallel to it, Figure 2. The defects were 13.6 and 9.2mm in depth for the BIMET01 and 02 specimens respectively. Other geometrical characteristics are included in Figure 2.

Tests were performed in four-point bending at ambient temperature in a 5MN test machine operating under displacement control. Figure 3 illustrates the moment, $M_{app}$, versus crack-mouth opening displacement (CMOD) behaviour of each test. BIMET01 achieved a maximum bending moment, $M_{max}$, of 180 kNm prior to unloading whilst that for BIMET02 was 220 kNm. The initiation moment, $M_i$, was estimated from electrical potential drop data as between 142 and 154 kNm for BIMET01 (Figure 4) and between 155 and 170 kNm for BIMET02. Subsequent ductile tearing of up to 1.4 mm in BIMET01 and up to 8.7 mm in BIMET02 occurred along the buttering/ferritic steel interface. A comprehensive evaluation of residual stresses was performed by measurements of residual strains based on neutron diffraction, Figure 5, and numerical simulation of the DMW fabrication.

## R6 ANALYSES

The R6 procedure [1] provides a basis for defect assessment with respect to two failure conditions: fracture and plastic collapse. Assessments are performed with respect to a failure assessment diagram (FAD), in which the abscissa is defined as $L_r = M_{app}/M_L$, where $M_L$ is the limit moment. Under primary and secondary loading, the ordinate, $K_r$, is defined as

$$K_r = \left\{\left(K^P_{eff} + K^S_{eff}\right)/K_{mat}\right\} + \rho \qquad (1)$$

where $K^P_{eff}$ and $K^S_{eff}$ are effective stress intensity factors, accounting for mixed-mode loading, under primary and secondary loading respectively; $K_{mat}$ is the material fracture toughness and $\rho$ is a plasticity correction parameter. On the FAD, the failure assessment point, plotted for the defect/structure of interest is compared with a failure assessment curve which defines the failure condition. The structure is deemed to be "safe" when the assessment point is located inside the curve. The following sub-sections describe the basis of the R6 analyses performed for the BIMET01 and 02 tests.

### *Evaluation of $K^P_{eff}$ and $K^S_{eff}$*

The variation of $K^P_{eff}$ with $M_{app}$ was calculated using a weight function solution for a pipe containing an external semi-elliptical defect [2]. This method yielded $K^P_{eff} = 0.635M_{app}$ for BIMET01 and $K^P_{eff} = 0.486M_{app}$ for BIMET02, with $K^P_{eff}$ in MPa$\sqrt{m}$ and $M_{app}$ in kNm. A more accurate solution was obtained from a large-strain elastic-plastic finite element analysis (FEA) of BIMET01 [3]. This gave $K^P_{eff} = 0.652M_{app}$. Since a FEA of BIMET02 was unavailable, the weight function result was scaled by the ratio of BIMET01 solutions to provide a more accurate solution for this test. The value of $K^s_{eff}$ was calculated using measured residual stress data, Figure 5, in conjunction with tabulated weight function coefficients [2]. The Mode I, II and III stress intensity factors thus calculated were combined to give $K^s_{eff}$

using usual sum-of-squares relationship. This gave $K_{eff}^{s}$ equal to 33.0MPa√m for BIMET01 and 29.2MPa√m for BIMET02.

***Evaluation of ρ***

The plasticity correction ρ was calculated according to the procedure set out in R6 Section II.6 [1]. Here, ρ is defined according to the following expression:

$$\rho = \Psi - \Phi\left\{\left(K_I^s / K_p^s\right) - 1\right\} \qquad (2)$$

where Ψ and Φ are tabulated functions of the parameter $K_p^s/(K_I^P/L_r)$, $K_p^s$ is the effective stress intensity factor due to secondary loading, $K_I^P$ and $K_I^s$ are the Mode I stress intensity factors due to primary and secondary loading respectively.

***Evaluation of $K_{mat}$***

The results of three Mode I fracture toughness tests for the 308L weld metal buttering were used to define a power-law J R-curve as: $J = 262\ \Delta a^{0.4342}$ [4], with J defined in kJ/m$^2$ and ductile crack extension, Δa, defined in mm. The initiation condition was considered to lie between Δa = 0.2 and 0.5mm, i.e. between J = 130 and 194 kJ/m$^2$. These values of J were converted to K using the plane strain small-scale yielding expression $K^2 = E'J$, where $E' = E/(1-\nu^2)$, E being Young's modulus and ν being Poisson's ratio. R6 assessments were thus carried out with $K_{mat}$ = 156MPa√m (Δa = 0.2mm) and 190MPa√m (Δa = 0.5mm).

***Evaluation of limit moment***

The limit moment, $M_L$ for each test was derived in three ways. First, the solution for a part-penetrating circumferential defect under bending in Miller's Limit Load Handbook [5] was used. Here, the limit moment is defined as:

$$ML = m \cdot (4R^2 t\sigma_y) \qquad (3)$$

where m is a function of the crack geometry. The limit moment was calculated with the yield stress, $\sigma_y$, equal to that of the 304 base material, giving $M_L$ = 128kNm for BIMET01 and 139kNm for BIMET02. Secondly, a FEA was used to calculate $M_L$ for BIMET01, based on the strength properties of the weaker type 304 stainless steel base material. The limit moment was calculated as 150kNm. This value was scaled by the ratio of Miller limit moments to give a value of 162kNm for BIMET02. Finally, using the ASME 'twice the elastic slope' method alongside a second FEA [2], the mismatch limit moment ($M_{L,mis}$) for BIMET01, incorporating all materials, was estimated to be 160 kNm. This result was again scaled by the ratio of Miller limit moments to give a value of 174kNm for BIMET02.

In the R6 analyses, the base material limit moment, $M_{L,b}$ was taken as either 128 or 150kNm and the mismatch limit moment, $M_{L,mis}$, as 160kNm for BIMET01. For BIMET02, $M_{L,b}$ was taken as either 139 or 162kNm and the mismatch limit moment, $M_{L,mis}$, as 174kNm.

***Weld mismatch***

The effects of weld mismatch were assessed with reference to the procedures of R6 Section III.8. The stress-strain curve for the equivalent material was calculated using the ratio ($M_{L,mis}/M_{L,b}$) and the 'mismatch' ratio $M = (\sigma_{y,w}/\sigma_{y,b})$. Here $\sigma_{y,w}$ was referred to the 308L-buttering/filler weld, and $\sigma_{y,b}$ to the 304 base material. The ratio of the limit moments was 160/150 = 1.067, and M = 403/297 = 1.36. The resultant equivalent material curve was used to define an Option 2 curve.

***Failure assessment curves***
R6 assessments were performed with respect to three failure assessment curves: (i) Option 1 curve, (ii) Option 2 curve based on 304 material properties and (iii) Option 2 curve based on the equivalent material properties, Figure 6.

## RESULTS

***Assessment of crack initiation***
BIMET01 (Figure 7): The Option 1 assessment for primary plus secondary loading using the Miller limit moment gives $112 < M_i < 123$kNm for $0.2 < \Delta a < 0.5$mm. This is significantly lower than the experimentally determined range. Reference to the limit moment derived by FE analysis gives $M_i$ in the range 123 to 136kNm while reference to the Option 2 failure assessment curve indicates that the assessed initiation moment lies between 138 and 149 kNm. The equivalent material assessment gives an estimated initiation moment between 144 and 156kNm.

BIMET02 (Figure 8): The Option 1 assessment using the Miller limit moment gives $131 < M_i < 141$kNm for $0.2 < \Delta a < 0.5$mm. This is again lower than the experimentally determined range. Use of the limit moment derived by FE analysis gives $M_i$ in the range 145 to 158kNm while reference to the Option 2 failure assessment curve indicates that the assessed initiation moment lies between 160 and 167kNm. The equivalent material assessment gives an estimated initiation moment between 168 and 175kNm.

***Assessment of tearing instability***
Tearing instability during each test was assessed via an R6 Category 3 analysis. The solutions for crack driving force and $M_{L,mis}$ were updated for crack growth ($\Delta a$) by scaling the original values ($\Delta a = 0$) in terms of the relevant K and limit moment solutions given in [2] and [5], respectively. Values of $K_{mat}(a+\Delta a)$ were based on the tearing toughness curve for the 308L material. The predicted instability moment was 159kNm for BIMET01 and 180kNm for BIMET02. These results underestimate the experimentally observed values of $M_{max} \sim 180$ and 200kNm, respectively.

## DISCUSSION

The choice of limit moment has a noticeable influence on the assessed value of $M_i$. Use of the Miller solution provides a highly conservative assessment of $M_i$ that is more than 20 % below the mean value deduced from EPD measurements. By comparison, use of the FEA solution gives a value of $M_{L,b}$ which is ~ 17 % higher than Miller's solution, and yields a value of $M_i$ which is approximately 15 % below the mean value. The maximum assessed values of $M_i$ correspond to the Option 2 analyses for an equivalent material. The assessments referenced to $J_{0.2}$ fall within the experimentally determined range.

It is evident that the limit moment behaviour of the DMW is controlled by the strength of the weaker material – i.e. the type 304 stainless steel. The effect of weld mismatch is determined primarily by the mismatch in strength between the 308L-buttering and filler weld and the 304 base material.

The choice of failure assessment curve (Option 1 vs. Option 2) has a significant influence on the assessed value of $M_i$. Whilst the Option 1 curve provides a value of $M_i \sim 15$ % below the mean experimental value, with the Option 2 curve the corresponding reduction is ~ 2 %.

The influence of using equivalent material properties rather than those of the weaker type 304 stainless steel was modest in the present work. A comparison of results from the various Option 2 analyses for primary + secondary loading suggests a 4 % increase in $M_i$ that is mainly attributable to the increase in limit moment from $M_{L,b}$ to $M_{L,mis}$.

Lastly, the R6 analyses suggest that residual stress influenced crack initiation during both tests. This is despite the fact that assessed values of $M_i$ correspond to values of $L_r$ close to unity.

## CONCLUSIONS

1. The choice of limit moment has a noticeable influence on the assessed value of $M_i$. The limit moment behaviour of the DMW is controlled by the strength of the weakest material.
2. The choice of failure assessment curve has a significant influence on the assessed value of $M_i$, with Option 2 curves providing less conservative assessments.
3. Residual stress influences the initiation of crack growth despite assessed values of $M_i$ corresponding to $L_r \approx 1$ where the influence of such stresses would be expected to be small.
4. The influence of using equivalent material properties rather than those of the weaker type 304 stainless steel base material was found to be modest in the present work.
5. The R6 assessments of initiation (based on 0.2 mm tearing) and tearing instability were conservative with respect to the experimental results for both BIMET01 and 02 tests.

## ACKNOWLEDGEMENTS

This work was undertaken within the context of a Euratom Framework Programme 1994-1998. The authors gratefully acknowledge funding from the CEC as well as matching and supplementary funding from the UK Health and Safety Executive. The technical contribution of all BIMET partners and also Dr R A Ainsworth (British Energy Generation Ltd) is also acknowledged.

## REFERENCES

1. R/H/R6 Revision 4, “Assessment of the integrity of structures containing defects”, British Energy Generation Ltd, May 2001.
2. B Drubay, S Chapuliot and M Lacire, “A16: Guide for defect assessment and leak before break analysis”, CEA Report, 1999.
3. Goldthorpe, M. R. and Wiesner, C. S., “BIMET – Structural integrity of bi-metallic components: three-dimensional finite element analysis of test BIMET01”, TWI Report No. 8294/3A/99, 1999.
4. P Nevasmaa, “BIMET fracture toughness curves”, email with accompanying spreadsheet to BIMET Task Group 5 participants, VTT Manufacturing Technology, Espoo, Finland, 25 February 1999.
6. A G Miller, “Review of limit loads of structures containing defects”, Int. J. Pres. Vessels Pip, Vol. 32, pp. 197-327, 1988.

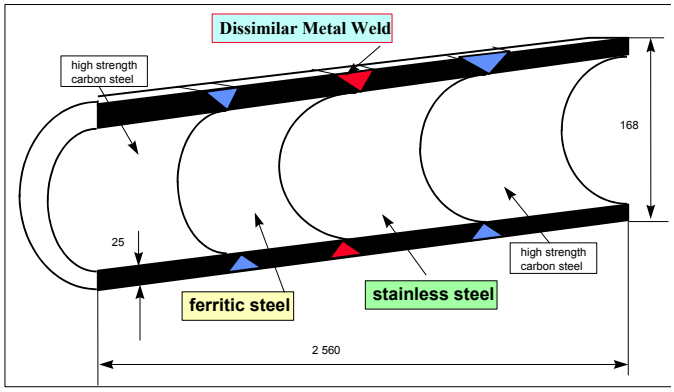


**Figure 1:** BIMET01 and 02 specimen geometry

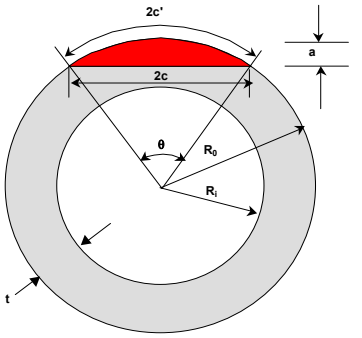


| | BIMET01 | BIMET02 |
|---|---|---|
| $R_0$ (mm) | 84 | 84 |
| $R_i$ (mm) | 59 | 59 |
| t (mm) | 25 | 25 |
| $a_{actual}$ (mm) | 13.8 | 9.28 |
| a (mm) | 12.5 | 8.33 |
| a/ t | 0.5 | 0.33 |
| 2c' (mm) | 93 | 75.5 |
| 2c (mm) | 88.2 | 73.0 |
| θ (°) | 63.3 | 51.5 |
| $R_i / R_0$ | 0.70 | 0.70 |
| $R_{mean}$ (mm) | 71.5 | 71.5 |

**Figure 2:** BIMET01 and 02 defect geometry

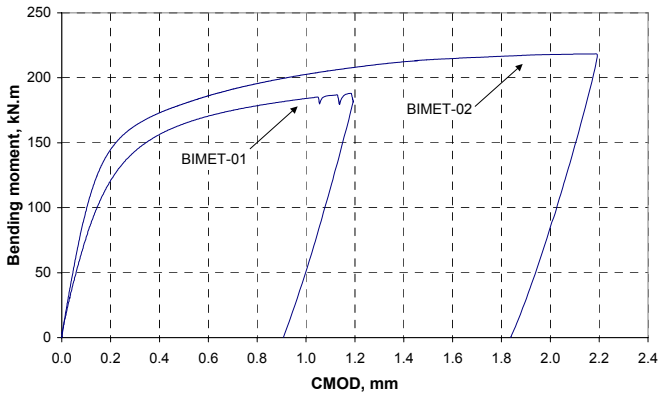


**Figure 3:** Load-displacement behaviour

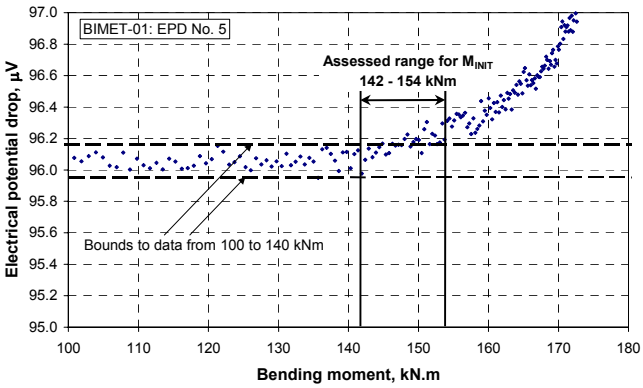


**Figure 4:** Assessment of initiation moment

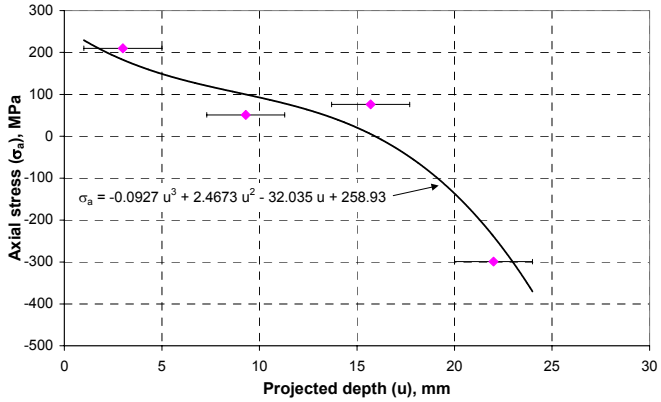


**Figure 5:** Axial residual stress profile

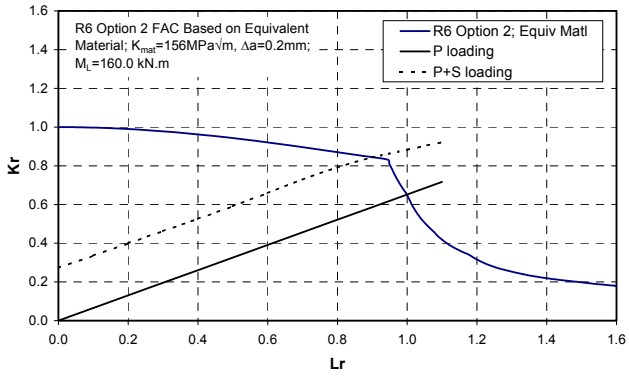


**Figure 6:** Option 2 FAD for BIMET01

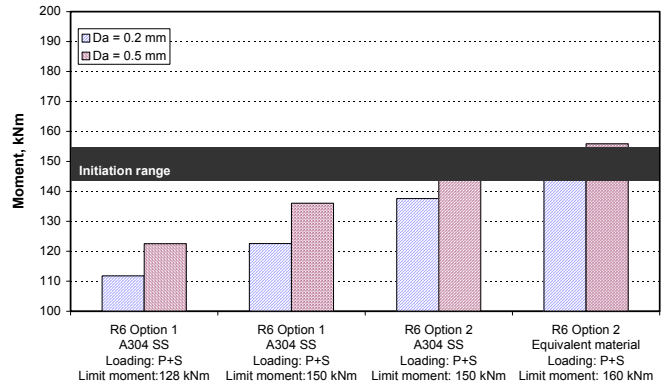


**Figure 7:** Summary of results of R6 analyses to calculate initiation moment: BIMET01

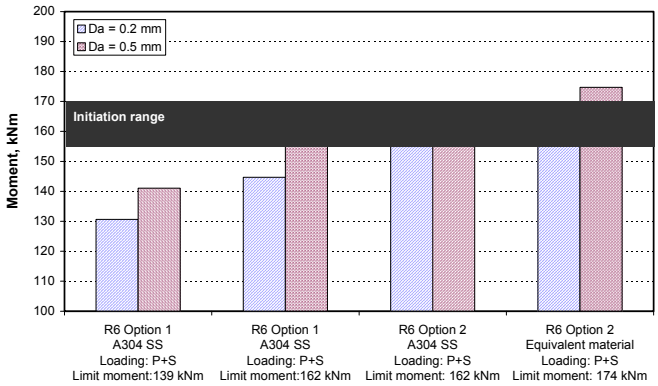


**Figure 8:** Summary of results of R6 analyses to calculate initiation moment: BIMET02